

Resonance production in p+p, p+A and A+A collisions measured with HADES

M. Lorenz^{7,a}, G. Agakishiev⁶, C. Behnke⁷, D. Belver¹⁶, A. Belyaev⁶, J.C. Berger-Chen⁸, A. Blanco¹, C. Blume⁷, M. Böhmer⁹, P. Cabanelas¹⁶, C. Driksa¹⁰, A. Dybczak², E. Eppel⁸, L. Fabbietti^{8,9}, P. Fonte^{1,a}, J. Friese⁹, I. Fröhlich⁷, T. Galatyuk^{4,b}, J. A. Garzón¹⁶, K. Gill⁷, M. Golubeva¹¹, D. González-Díaz⁴, F. Guber¹¹, M. Gumberidze¹⁴, S. Harabasz⁴, T. Hennino¹⁴, R. Holzmann³, P. Huck⁹, C. Höhne¹⁰, A. Ierusalimov⁶, A. Ivashkin¹¹, M. Jurkovic⁹, B. Kämpfer^{5,c}, T. Karavicheva¹¹, I. Koenig³, W. Koenig³, B. W. Kolb³, G. Korcyl², G. Kornakov¹⁶, R. Kotte⁵, A. Krása¹⁵, E. Krebs⁷, F. Krizek¹⁵, H. Kuc^{2,14}, A. Kugler¹⁵, A. Kurepin¹¹, A. Kurilkin⁶, P. Kurilkin⁶, V. Ladygin⁶, R. Lalik⁸, S. Lang³, K. Lapidus⁸, A. Lebedev¹², L. Lopes¹, L. Maier⁹, A. Mangiarotti¹, J. Markert⁷, V. Metag¹⁰, J. Michel⁷, C. Müntz⁷, R. Münzer⁸, L. Naumann⁵, M. Palka², Y. Parpottas^{13,d}, V. Pechenov³, O. Pechenova⁷, J. Pietraszko⁷, W. Przygoda², B. Ramstein¹⁴, L. Rehnisch⁷, A. Reshetin¹¹, A. Rustamov⁷, A. Sadovsky¹¹, P. Salabura², T. Scheib⁷, H. Schuldes⁷, J. Siebenson⁸, Yu.G. Sobolev¹⁵, S. Spataro^e, H. Ströbele⁷, J. Stroth^{7,3}, P. Strzempek², C. Sturm³, O. Svoboda¹⁵, A. Tarantola⁷, K. Teilab⁷, P. Tlusty¹⁵, M. Traxler³, H. Tsertos¹³, T. Vasiliev⁶, V. Wagner¹⁵, M. Weber⁹, C. Wendisch^{5,c}, J. Wüstenfeld⁵, S. Yurevich³, Y. Zanevsky⁶

- ¹ LIP-Laboratório de Instrumentação e Física Experimental de Partículas , 3004-516 Coimbra, Portugal
- ² Smoluchowski Institute of Physics, Jagiellonian University of Cracow, 30-059 Kraków, Poland
- ³ GSI Helmholtzzentrum für Schwerionenforschung GmbH, 64291 Darmstadt, Germany
- ⁴ Technische Universität Darmstadt, 64289 Darmstadt, Germany
- ⁵ Institut für Strahlenphysik, Helmholtz-Zentrum Dresden-Rossendorf, 01314 Dresden, Germany
- ⁶ Joint Institute of Nuclear Research, 141980 Dubna, Russia
- ⁷ Institut für Kernphysik, Goethe-Universität, 60438 Frankfurt, Germany
- ⁸ Excellence Cluster 'Origin and Structure of the Universe' , 85748 Garching, Germany
- ⁹ Physik Department E12, Technische Universität München, 85748 Garching, Germany
- ¹⁰ II.Physikalisches Institut, Justus Liebig Universität Giessen, 35392 Giessen, Germany
- ¹¹ Institute for Nuclear Research, Russian Academy of Science, 117312 Moscow, Russia
- ¹² Institute of Theoretical and Experimental Physics, 117218 Moscow, Russia
- ¹³ Department of Physics, University of Cyprus, 1678 Nicosia, Cyprus
- ¹⁴ Institut de Physique Nucléaire (UMR 8608), CNRS/IN2P3 - Université Paris Sud, F-91406 Orsay Cedex, France
- ¹⁵ Nuclear Physics Institute, Academy of Sciences of Czech Republic, 25068 Rez, Czech Republic
- ¹⁶ LabCAF. Dpto. Física de Partículas, Univ. de Santiago de Compostela, 15706 Santiago de Compostela, Spain

Abstract. The knowledge of baryonic resonance properties and production cross sections plays an important role for the extraction and understanding of medium modifications of mesons in hot and/or dense nuclear matter. We present and discuss systematics on dielectron and strangeness production obtained with HADES

on p+p, p+A and A+A collisions in the few GeV energy regime with respect to these resonances.

1 Introduction

The dynamical generation of hadron masses is one of the great topics of nuclear physics nowadays. The underlying QCD symmetry responsible for the masses is called chiral symmetry and is spontaneously broken in the vacuum but expected to be (partially) restored inside a dense and/or hot nuclear medium [1]. Most promising experimental observables of this restoration are the decays of medium modified short lived vector mesons via a virtual photon into a dilepton pair, as the decay products only experience small final state interaction and hence deliver the undistorted information to the detectors [2].

However, the connection between a distorted QCD vacuum and specific particle properties is not straightforward and can at the moment not be clearly defined. Therefore, hadronic models, which take the modification of the meson spectral function -due to its coupling via resonances to the surrounding medium- into account, are needed to predict specific particle properties for given nuclear densities and temperatures [3].

Experimentally, dilepton measurements are extremely challenging as apart from the small branching ratio of the electromagnetic decay of order 10^{-4} and huge combinatorial background, one has to disentangle several broad and overlapping contributions in the reconstructed spectrum. Clearly in order to find a modification of one specific source all other contributing sources must be under control.

Moreover, it was realized that even in p+p collisions particle production via intermediate resonances can modify the Breit-Wigner shape of short lived particle states like for example the ρ meson mainly due to kinematical constraints [4–6]. These modifications can hardly be disentangled from medium modification of spectral functions in hadronic models or the restoration of chiral symmetry as in all cases the presence of baryons are at the origin of such changes. Therefore, systematic and accurate measurements are needed, in order to get a, as far as possible, complete picture.

2 HADES

HADES is a fixed-target, high-acceptance and multi-propose spectrometer capable of measuring dielectron as well as hadron observables. The physics program ranges from HIC over elementary n+p and p+p collisions up to pion and proton induced reactions on heavy nuclei (cold nuclear matter). It is located at the Helmholtzzentrum für Schwerionenforschung (GSI) in Darmstadt which provides already now high intensity ion (10^8 ions/s) and proton beams at energies up to 3.5 A GeV and will be extended to higher beam intensities (up to 10^{12} ions/s) and energies (35 A GeV) with the upcoming FAIR facility.

The key features of the apparatus, see Fig. 1, are its huge geometrical acceptance covering the full azimuthal angle and polar angles from 18° to 85° . The time resolution is around 90 ps while the momentum resolution for electrons is 1.5% at 0.5 GeV/c momentum. The detectors can be read out fast with a peak rate of up to 50 kHz. While hadrons are identified based on the time of flight measurement and on the energy-loss information in the tracking detectors and the time-of-flight walls, for electrons additional identification power is gained by dedicated RICH and SHOWER detectors. A detailed description can be found in [7].

^a e-mail: Lorenz@physik.uni-frankfurt.de

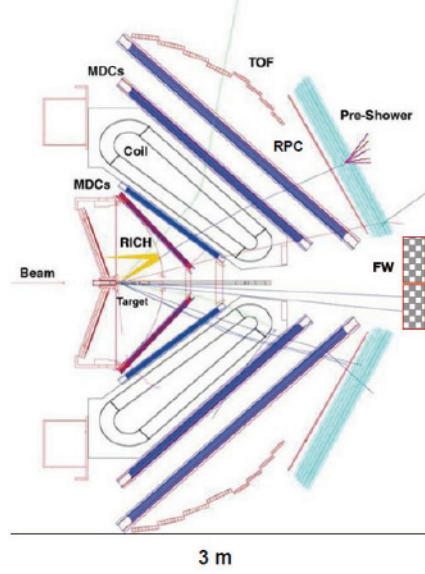


Fig. 1. Cross section of the HADES detector. The beam impinges on a segmented target which is surrounded by a RICH detector for electron/positron identification. The magnet spectrometer consists of two double layers of drift chambers in front of and behind a toroidal magnetic field. The field geometry is chosen in order to provide field free regions for the detectors. At the end of the apparatus two scintillator time of flight walls and at low polar angles an electromagnetic pre-shower detector are placed.

3 Dielectron radiation

3.1 Elementary p+p collisions @ 3.5 GeV/c

One distinguishes between two subcategories of hadron decays in the dielectron spectrum, two-body and multi-body (Dalitz) decays. In the low invariant mass region below $0.15 \text{ GeV}/c^2$ of the spectrum mainly Dalitz decays of neutral pions contribute. The intermediate part of the spectrum from $0.15 \text{ GeV}/c^2$ to $0.47 \text{ GeV}/c^2$ is dominated by Dalitz decays of η mesons and weaker contributions of baryonic resonances. In the region between $0.47 \text{ GeV}/c^2$ and $0.7 \text{ GeV}/c^2$ direct ρ decays and Dalitz decays of baryonic resonances contribute, while the region above $0.7 \text{ GeV}/c^2$, is dominated by direct decays of vector mesons.

In the following, the data will be compared to a tuned version of the high energy event generator PYTHIA. Although PYTHIA is usually used to describe particle production in the high energy regime ($\sqrt{s} > 10 \text{ GeV}$) and generates particles according to a quark and antiquark string fragmentation model (Lund model), it was shown in [8] that by a parameter adjustment a satisfactory description of p+p reactions at 3.5 GeV can be achieved. The decay of hadrons contributing to the dielectron spectrum is modeled by the PLUTO event generator [9]. The cross sections of the long-lived sources, the Dalitz decays of π^0 and η mesons as well as the direct decay of ω mesons, are estimated by fitting the simulated contributions to the measured yield in the corresponding regions, where the respective sources dominate the dielectron spectrum. The contribution from the ω Dalitz decay is fixed by its known branching ratio and the defined cross section of its direct decay channel. The decay of the pseudoscalar (π^0 , η) and vector meson Dalitz decays are adopted according to [10] including electromagnetic transition form factors. The transition form factors used for the direct vector mesons decays are based on the vector meson dominance model (VMD) [11].

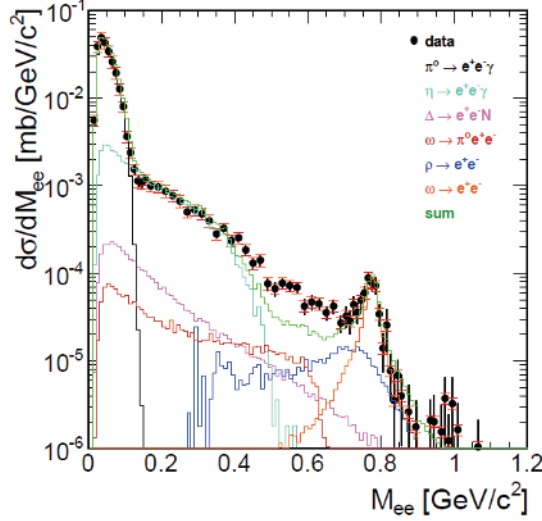


Fig. 2. Comparison of p+p data to a calculated PYTHIA/PLUTO dielectron cocktail. The different sources are displayed on the upper right side of the figure. While the description is in good agreement with the data in most parts of the spectrum, strong deviations in the invariant mass region from 0.5 to 0.7 GeV/c^2 are visible.

The contributions of short-lived sources like the ρ and Δ are much more difficult to constrain. The dielectron yield originating from Δ Dalitz decays can only be roughly constrained by the invariant mass distribution at the shoulder of the η contribution around 0.5 GeV/c^2 and on the right side of the peak structure of the direct ω decay at masses larger than 0.85 GeV/c^2 . The dielectron yield of the direct decays of the ρ meson can be constrained on both sides of the ω peak, which complicates the situation since also Δ Dalitz decays contribute in both regions. Additional constraints, especially in case of the Δ can be gained from the momentum distributions, which differ strongly for the different sources.

Following this discussion, it is clear that for fixing at the same time several overlapping broad contributions at different points in the spectrum a solid knowledge of their shape is of eminent importance.

Unfortunately the knowledge on the pattern of dielectron emission from broad resonances is very limited and has to be guessed to some extent. It depends on several parameters and most of them can only be approximately constrained by data or theory up to now:

- **Mass dependent width and branching ratio:** The masses of the Δ and ρ are generated according to relativistic Breit-Wigner distributions including a mass dependent total width $\Gamma_{tot}(m)$. In case of the Δ the mass dependence is calculated by its dominant decay channel to $\pi+N$ according to:

$$\Gamma_{tot}(m) \simeq \Gamma_{\Delta \rightarrow \pi N} = \Gamma_{pole} \frac{m_{pole}}{m} \left(\frac{q}{q_{pole}} \right)^{2L+1} \cdot F_{cutoff}, \quad (1)$$

with Γ_{pole} , m_{pole} and q_{pole} representing the Δ width, mass and the pion momentum in the Δ rest frame at the resonance pole, while $L=1$ is the quantum number of the orbital momentum and F_{cutoff} , the cut off parameter which will be discussed in the next item. The momentum term reflects the decrease of the decay probability towards small momenta, due to the fact that the pion must be generated at increasingly large distance from the nucleon in order to conserve the angular momentum.

The mass dependent branching ratio $\frac{\Gamma_{\Delta \rightarrow \pi N}}{m}$ ¹ is taken according to [12] and was found to deliver more favorable results compared to other parametrization.

- **Cut off function:** For the mass states far above the resonance pole it is quite natural to assume that the probability to populate these states decreases asymptotically to 0. In literature several cut off parameterizations can be found [13,14]. All of them are in good agreement in the region around the pole which is well constrained by photo absorption and π^+ +p elastic scattering experiments. The asymptotic behavior however can only be guessed.² As cut-off the parametrization from [13]

$$F_{cutoff} \propto \frac{1}{q^2 + \delta^2}, \quad (2)$$

with $\delta^2 = 0.04 \text{ GeV}^2$ is used. The asymptotic resonance width is then proportional to the pion momentum q , which seems to be reasonable since it reflects phase space.

- **Electromagnetic transition form factors:** Depending on the 4-momentum transfer $q^2 = (\Delta E)^2 - (\Delta p)^2$ one defines the virtual photon to be space like or time like. If $q^2 > 0$ the photon mainly transfers energy and is called time like, while for $q^2 < 0$ mainly momentum is transferred and the photon is called space like. While in the space like region the electromagnetic transition form factors of the N - Δ transition are well constrained by data, no data and no solid theoretical parametrization exists for the time-like region. Therefore the magnetic form factor is approximated by its value at the photon point³, while the electric and Coulomb form factor terms are much smaller and neglected, like it is proposed in [12]. The transition form factors used for the direct vector meson decays, in particular the ρ , are based on the vector meson dominance model (VMD) [11] which on the other hand is based on the pion transition form factors.

The resulting dielectron cocktail compared to the data is shown in Fig. 2. The cocktail describes the spectrum with fair agreement apart from the region between the η shoulder and the direct ω decay peak structure from $\approx 0.5 \text{ GeV}/c^2$ to $\approx 0.7 \text{ GeV}/c^2$. The strength of the Δ contribution is mainly constrained by the transverse momentum P_t of the dielectron [4]. A better description may be achieved by changing either the shape of the ρ or the Δ contribution e.g. by coupling the ρ to the Δ resonance using a different parametrization of the transition form factor or by introducing higher lying resonance which couple via the ρ (VMD) to the virtual photon. Indeed the up to now best description of the data (M_{ee} , as well as P_t and Y_{ee}) is achieved by using a version of the GiBUU which includes this coupling of the ρ to higher lying resonances [5]. This results in a strong modification of the shape of the ρ meson. This modification can be understood first of all by the underlying reaction which changed from

$$NN \rightarrow NN\rho \quad (3)$$

to

$$NN \rightarrow NR \rightarrow NN\rho. \quad (4)$$

In the latter one the available phase space for the ρ meson is smaller, thus the low mass part of the ρ is populated more strongly. Secondly, this effect is enhanced by contributing resonances like the $D_{13}(1520)$ with pole masses below the $N+\rho$ threshold which favorably populate the low mass part of the ρ . However the question arises whether it makes then sense anymore to

¹ Note that the branching ratio values listed by the PDG are always validated around the pole mass and are expected to change as a function of the mass. The effect can easily be illustrated by moving away from the pole mass below the threshold of the dominant decay channel at the pole, where the branching ratio will clearly change strongly. Moreover, the branching ratio, the widths and the lifetime of a particle are entangled on the quantum level, which might cause unpredictable effects.

² The question becomes even philosophic if one moves so far away from the pole that the actual mass value already agrees with the pole mass of the next higher lying resonance with equal quantum numbers, e.g. $\Delta(1232)$ and $\Delta(1600)$.

³ real photon with $m=0$

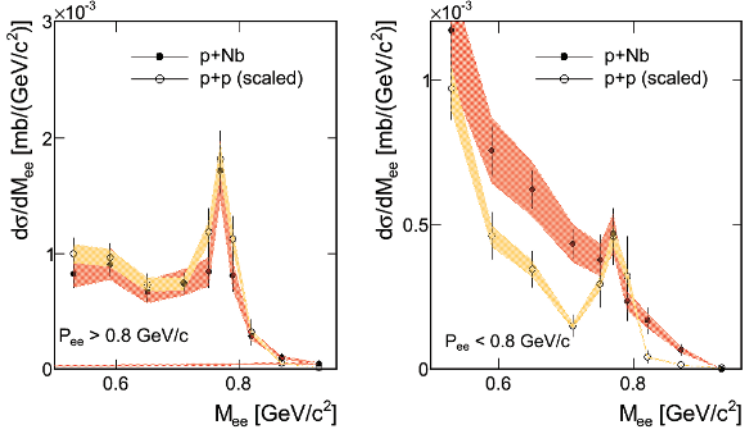


Fig. 3. Comparison of the dielectron invariant mass spectra in the vector meson mass region for pairs with $P_{ee} > 0.8$ GeV/c from p+p (scaled) and p+Nb at a kinetic beam energy of 3.5 GeV. Within errors the two spectra overlap. Right: For pairs with $P_{ee} < 0.8$ GeV/c a clear difference in shape is visible.

distinguish between the ρ and baryonic resonance contributions as they are strongly coupled anyhow.

3.2 Cold nuclear matter and HIC

Due to the problems in the theoretical description of the dielectron yield we focus on the comparison to elementary data in this paper. According to the systematics on dielectron emission obtained in p+p and d+p collisions at various beam energies by the DLS collaboration [15] it is safe to conclude that at the kinetic beam energy of 3.5 GeV isospin effects play only a secondary role. Therefore in order to extract medium effects in p+Nb the above discussed p+p data at the same kinetic beam energy of 3.5 GeV/c is a valuable reference.

According to hadronic models, possible modifications should be most pronounced for relative momenta to the medium smaller than 0.8 GeV/c. As this region is experimentally challenging to access, the current data represent the first measurement of induced dielectron emission from cold nuclear matter in this kinematic region and should be therefore more sensitive to these changes than previous experiments.

We compare the shape in the invariant mass spectra separately for pairs from p+Nb collisions with momenta larger and smaller 0.8 GeV/c to the p+p data in the same kinematic regions scaled to the number of participants and the total reaction cross section. While for pairs with $P_{ee} < 0.8$ GeV/c no significant difference in the vector meson mass region within the systematic uncertainties indicated by the colored bands in the left side Fig. 3, is visible, the situation changes completely for small momenta: Here one observes a strong e^+e^- excess yield below the ω pole mass, as can be seen in the left panel of Fig. 3. Although the e^+e^- yield at the ω pole mass is not reduced, the underlying smooth distribution is enhanced, thus reducing the yield in the peak to almost zero within errors. Due to its large total width, the ρ meson is believed to be the dominating source for radiation from the medium. Therefore, we attribute the additional broad contribution to ρ -like channels. The observed decrease of the ω yield, compared to the p+p indicates that absorption of ω mesons dominates over feeding from secondary reactions. For more details, see [16].

Having this pronounced modification one would expect an even stronger one, when moving to HIC. Indeed, comparing the dielectron yield from Ar+KCl collisions at a kinetic beam energy of 1.76 A GeV, normalized to the neutral pion multiplicity, in the invariant mass region

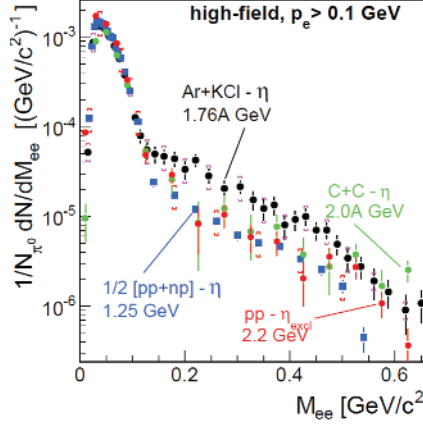


Fig. 4. Comparison of the dielectron yield in Ar+KCl to various reference, each normalized to the neutral pion production yield.

between 0.15 GeV/c and 0.5 GeV to various reference spectra a strong excess is observed, see Fig. 4 (the energy dependence is taken out to some extent due to the normalization). Note that the comparison to various references is needed at this energy due to possible isospin effects, moreover a detailed comparison in the vector meson mass region is unfortunately hampered by low statistics. In the region of the excess one expects a strong contribution of baryonic resonance (compare the calculated dielectron cocktail in Fig. 2). However, following our line of argumentation it is questionable whether one can clearly distinguish between baryonic resonance and ρ contributions. In this sense, the emerging picture would be a suppression of particle like states (ω -meson) in favor of broad baryonic/ ρ -like contribution inside the medium. However it is clear that for a more solid understanding of these modifications it is of paramount to better control the different resonance contribution e.g. $\Delta(1232)$, $N(1520)$ and $N(1535)$. At least their relative contribution in the p+p data will be constrained by an exclusive channel analysis of HADES data expected to be finalized within this year.

4 Strangeness production

The understanding of resonances containing strangeness is of great importance for the understanding of the \bar{K} -N potential, which can be extracted by comparing transverse momentum spectra to transport models [18]. However before doing so, the properties and production rates of those resonances have to be under control, as they might modify the measured momentum distribution either by late decays as shown in [19], or by direct coupling of the meson to the resonances inside the medium, similar to the case of the vector mesons.

For the later one the $\Lambda(1405)$ is considered to be a major player as it's pole mass lies slightly below the \bar{K} -N threshold. Theoretically the $\Lambda(1405)$ is treated within a coupled channel approach, based on chiral dynamics. In this ansatz it is dynamically generated by superpositions of different states with the excitation either in the meson cloud or in the quark core. To constrain the different contributions the only experimental observable below the \bar{K} -N threshold is the spectral shape of this resonance extracted from its decays to a $\Sigma\pi$ state.

Based on the analysis of the reaction $p+p \rightarrow p+K^+(\Sigma+\pi)^0$ at 3.5 GeV kinetic beam energy, HADES has measured the first data on the decay of the $\Lambda(1405)$ resonance into charged final states. The spectral shape, the polar production angle, and the production cross-section could be extracted in [20]. The efficiency and acceptance-corrected missing mass distribution shows a peak structure clearly below 1.4 GeV/c². The best agreement between data and simulation

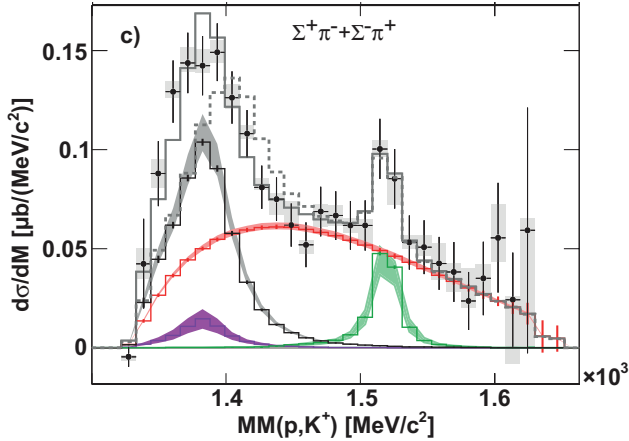


Fig. 5. Efficiency and acceptance-corrected missing mass distribution of the proton and the K^+ . The best agreement between data and simulation (gray histogram, solid line) is obtained by simulating the $\Lambda(1405)$ as a relativistic s-wave Breit-Wigner distribution with a width of $50 \text{ MeV}/c^2$ and a pole mass of $1385 \text{ MeV}/c^2$. In addition the contributions of $\Lambda(1520)$ (green), $\Sigma(1385)$ (purple) and non resonant $\Sigma\pi$ (red) production are displayed.

(gray histogram, solid line, Fig. 5) is obtained by simulating the $\Lambda(1405)$ as a relativistic s-wave Breit-Wigner distribution with a width of $0.05 \text{ GeV}/c^2$ and a pole mass of $1.385 \text{ GeV}/c^2$. Using instead the nominal mass of $1.405 \text{ GeV}/c^2$ results in the gray dashed histogram which fails to describe the experimentally observed peak structure. In addition the contributions of $\Lambda(1520)$ (green), $\Sigma(1385)$ (purple) and non resonant $\Sigma\pi$ (red) production obtained by full scale simulation and carefully tested by various consistency checks, are displayed in Fig. 5. The analysis of its polar angle distribution suggests that the $\Lambda(1405)$ is produced isotropically in the p-p center of mass system.

References

1. R. Brockmann and W. Weise, Phys. Lett. **B 367**, (1996) 46
2. R. Rapp and J. Wambach, Adv. Nucl. Phys. **25** (2000) 1
3. S. Leupold, V. Metag, and U. Mosel, Int. J. Mod. Phys. **E 19**, (2010) 147-224
4. G. Agakishiev et al. (HADES Collaboration), Eur.Phys.J. **A 48** (2012) 64
5. J. Weil, H. van Hees, and U. Mosel, arXiv:1203.3557 [nucl-th]
6. D. Schumacher, S. Vogel and M. Bleicher, Acta Phys. Hung. **A 27** (2006) 451
7. G. Agakishiev et al. (HADES Collaboration), Eur. Phys. J. **A 41**, (2009) 243
8. J. Weil, K. Gallmeister and U. Mosel, arXiv:1105.0314 [nucl-th], (2011)
9. I. Frohlich et al., Eur. Phys. J. **A 45**, (2010) 401
10. L. G. Landsberg, Phys. Rep. **128** (1985) 301
11. G. Q. Li, C. M. Ko, G. E. Brown and H. Sorge, Nucl. Phys. A **611** (2011) 539
12. M. I. Krivoruchenko and A. Faessler, Phys. Rev. D **65** (2001) 017502
13. D. M. Manley and E. M. Saleski, Phys. Rev. D **45** (1992) 4002
14. J. H. Koch, E. J. Moniz and N. Ohtsuka, Ann. Phys. D **154** (1984) 99
15. W.K. Wilson et al. (DLS Collaboration), Phys. Rev. **C57** (1998) 1865-1878
16. G. Agakishiev et al. (HADES Collaboration), arXiv:1205.1918 [nucl-ex]
17. G. Agakishiev et al. (HADES Collaboration), Phys. Rev. **C84** (2011) 014902
18. G. Agakishiev et al. (HADES Collaboration) Phys. Rev. **C82** (2010) 044907
19. M. Lorenz et al. (HADES Collaboration), PoS BORMIO (2010) 038
20. G. Agakishiev et al. (HADES Collaboration), arXiv:1208.0205 [nucl-ex]